LAWRENCE
LIVERMORE
NATIONAL
LABORATORY

LLNL-CONF-425276

Nested high-resolution mesoscale/large eddy simulations in WRF: challenges and opportunities

J. D. Mirocha, G. Kirkil

March 9, 2010

The Fifth International Symposium on Computational Wind Engineering
Chapel Hill, NC, United States
May 23, 2010 through May 27, 2010

Disclaimer

The Fifth International Symposium on Computational Wind Engineering (CWE2010)
Chapel Hill, North Carolina, USA May 23-27, 2010

Nested high-resolution mesoscale/large eddy simulations in WRF: challenges and opportunities

Jeff Mirocha [a], Gokhan Kirkil [b]

[a]*Lawrence Livermore National Lab, Livermore, CA, USA, mirocha2@llnl.gov*
[b]*Lawrence Livermore National Lab, Livermore, CA, USA, kirkil1@llnl.gov*

ABSTRACT: The WRF model's grid nesting capability provides a potentially powerful framework for coupled simulations of flow covering a wide range of spatial and temporal scales, from large-scale weather features to atmospheric turbulence. As such, large-eddy simulations, which have traditionally relied upon idealized lateral boundary conditions, can be conducted on higher-resolution nests within mesoscale simulations, thereby obtaining inflow boundary conditions that incorporate upstream terrain and broader-scale meteorological variability. Such multiscale nested simulation provide a means for significant improvements of both site characterization, and of simulation of turbulent inflow properties experienced by wind turbines sited within the atmospheric boundary layer. While nesting has been widely and successfully applied at scales ranging from Global Climate Models to mesoscale numerical weather prediction resolutions (1000s to 1s of km), the WRF model's nesting behavior at higher resolution (less than 1 km) is poorly understood, with caveats beginning to appear in the literature and at conferences and workshops. Successful realization of WRF's multiscale flow capabilities and applications to detailed site characterization require that these caveats be articulated. We investigate WRF's grid nesting behavior at mesh resolutions near the mesoscale/LES interface to better understand how flow structures within the nested domain respond to errors contributed from the bounding solution and its transition across the nest interfaces. In particular we examine the roles of the turbulence subfilter models and surface boundary conditions by comparing simulations using many approaches from the literature, including linear and nonlinear, static and dynamic subfilter models, coupled with separate near-wall stress models. We will address the issues we have encountered using idealized simulations.

1 INTRODUCTION

The Weather Research and Forecasting model (WRF) is an atmospheric modeling system that can be employed to simulate flow at many different scales, ranging from the global circulation down to large-eddy simulation (LES), in which the energy-producing scales of three-dimensional atmospheric turbulence are resolved on the computational mesh (Skamarock et al. 2008). The WRF model also supports mesh refinement via grid nesting, which allows a portion of the computational domain to be simulated at higher mesh resolution, with the boundary conditions for the higher-resolution nest provided by the outer-domain solution. Such a grid nesting capability provides flexibility for many different applications, including, for example, mesoscale modeling and regional climate downscaling. The nesting capability likewise provides a framework within which LES can be conducted on a nested domain, with its lateral boundary conditions provided by a coarser-resolution mesoscale simulation (or cascade of such) performed on bounding domains. Such an approach could provide more realistic boundary conditions for LES than the idealized boundary conditions commonly employed, which typically exclude meteorological va-

riability, effects of upwind terrain, and the influence of physical processes such as radiation, cloud microphysics, which are contained in the WRF model's physics package.

While the computational framework for such simulations is provided by the WRF model (and other atmospheric models that support grid nesting), the conceptual framework for nesting LES inside of another simulation is less well established. Wyngaard (2004), Hatlee and Wyngaard (2007) and Kelly et al. (2009) present important discussions related to modeling the scales of motion between those for which LES is suitable, and those for which a large-scale PBL parameterization is appropriate. They have demonstrated a potential path forward by extending the scalar eddy diffusivity concept traditionally used in mesoscale modeling to a more general approach involving the solution of rate equations for the stresses and fluxes, applied in various contexts. Continued work in this direction will be required to provide appropriate closure models for use at scales too fine for mesoscale parameterizations but still too coarse for LES.

In addition to the above-discussed conceptual concerns, there are a number of practical impediments to effective nested LES, particularly involving transition of the flow across mesh interfaces and during its transport through the nested domain. LES inflow and interface conditions have been investigated by number of researchers (Keating et al., 2004, Piomelli et al., 2006). Recently, Vanella et al. (2008) tested the case of spatially developing isotropic turbulence advected past interfaces in LES simulations of channel flow where the grid is suddenly coarsened or refined. They discovered that a sudden discontinuity in filter width generates smaller errors than a gradual transition, which, by maintaining larger eddy viscosities, delays the generation of smaller scales of turbulence that can be resolved on the finer mesh. They also discovered that the use of a dynamic eddy viscosity subfilter-scale (SFS) stress model improve the numerical results around grid discontinuities relative to a simple, static linear eddy-viscosity SFS stress model.

The present study continues the above-described research by investigating the behavior and evolution of various flow parameters within the nested domain in nested large-eddy simulations using the WRF model. In particular, we demonstrate the profound influence of the turbulence SFS stress modeling approach on the flow properties of nest domain.

2 SFS MODELS FOR LES

The SFS stress in LES is defined as

$$\tau_{ij} = (\widetilde{u_i u_j} - \widetilde{u_i}\,\widetilde{u_j}) \tag{1}$$

Here, $\widetilde{u_i}$ are the resolved velocities, with $i,j = 1,2,3$ denoting the zonal (u), meridional (v), and vertical (w) components, with $i,j = 1,2,3$ indicating zonal (x), meridional (y), and vertical (z) components, respectively.

The commonly-employed static Smagorinsky (SS) SFS stress model (Smagorinsky, 1963; Lilly, 1967) is given by

$$\tau_{ij} = -2\vartheta_T \widetilde{S_{ij}}. \tag{2}$$

Here ν_T is the eddy viscosity coefficient, typically defined by

$$\nu_T = (C_S l)^2 \left|\tilde{S}\right|, \tag{3}$$

where C_S is a constant, l is a length scale which, in the WRF model, is given by $(\Delta x \Delta y \Delta z)^{1/3}$, where $\Delta x, \Delta y$ and Δz are the grid spacings in the x, y and z directions, respectively, $\widetilde{S_{ij}} = \frac{1}{2}\left(\frac{\partial \widetilde{u_i}}{\partial x_j} + \frac{\partial \widetilde{u_j}}{\partial x_i}\right)$ is the resolved strain-rate tensor, and $\left|\tilde{S}\right|$ is its magnitude.

The SS model relates the stress linearly to the strain rate through an eddy viscosity coefficient that can never take negative values, making the model absolutely dissipative, and overly dissipative near the surface. The appropriate value of C_S, which influences the rate of dissipation, is not widely agreed upon, with optimal values in the literature spanning a range from 0.1 to 0.25 depending upon the application. In this study we use the standard WRF value of $C_S = 0.23$.

One popular method for improving the SS model is to compute the value of C_S dynamically using the smallest-scale stresses that are well-resolved on the mesh. These stresses, denoted

$$L_{ij} = T_{ij} - \overline{\tau_{ij}} = \overline{\tilde{u}_i \tilde{u}_j} - \bar{\tilde{u}}_i \bar{\tilde{u}}_j \tag{4}$$

are computed using a filter, denoted by an overbar, both to project the solution onto a "coarsened" mesh, upon which the SFS stress field T_{ij} is computed, and to filter the SFS stress field computed for the explicit mesh. Using the SS closure given by Eqns. (2) and (3) as a model for the SFS stresses in Eqn. (4) yields

$$M_{ij} = 2\Delta^2 \left[\overline{|\tilde{S}|\tilde{S}_{ij}} - \alpha^2 \beta |\bar{\tilde{S}}| \bar{\tilde{S}}_{ij} \right]. \tag{5}$$

Here α represents the ratio of the coarse and fine mesh spacing, typically equal to 2, and β is a parameter that can account for scale dependence of C_S. The standard Dynamic Smagorisky model (DS, Germano et al, 1991) assumes scale-invariance, using $\beta = 1$, giving

$$C_S^2 = \frac{\langle L_{ij} M_{ij} \rangle}{\langle M_{ij} M_{ij} \rangle}. \tag{6}$$

An alternative to the scale-invariant formulation is to compute the scale dependence of C_S explicitly, using two different filters (with the second filter, denoted by a hat, typically twice the width of the first). This approach results in an analogous set of equations to those above:

$$Q_{ij} = \widehat{\tilde{u}_i \tilde{u}_j} - \hat{\bar{\tilde{u}}}_i \hat{\bar{\tilde{u}}}_j \tag{7}$$

$$N_{ij} = 2\Delta^2 \left[\widehat{|\tilde{S}|\tilde{S}_{ij}} - \alpha^2 \beta \left| \hat{\bar{\tilde{S}}} \right| \hat{\bar{\tilde{S}}}_{ij} \right] \tag{8}$$

$$C_S^2 = \frac{\langle Q_{ij} N_{ij} \rangle}{\langle N_{ij} N_{ij} \rangle} \tag{9}$$

Equations (6) and (9) yield two values for C_S, hence β which, with a power-law expression yields the appropriate value of C_S for the SFS stresses (Bou-zeid et al., 2005).

Dynamic SFS stress models are inherently unstable, leading to locally small or even negative values for the eddy viscosity coefficients, which can result in numerical instability. A commonly-employed approach is to average model quantities in homogeneous directions (Germano et. al., 1991; Porte-Agel et. al., 2000). However, for many flows, including those in complex terrain, homogeneous directions might not exist. An alternative is to average in a Lagrangian frame of reference, along fluid trajectories (Bou-Zeid et. al., 2005). This approach extends the averaging required to stabilize dynamic SFS stress models to flows over complex terrain (LASD).

While the DS and LASD models improve upon the SS model, the linear eddy viscosity closure assumption contains several deficiencies. The first is that the form of Eqn. (2) posits an improper alignment between the eigenvectors of the strain rate tensor of the flow and the modeled SFS stress tensor. In addition, those models do not properly account for backscatter (the inverse transfer of energy from small to large scales). While the SS model is absolutely dissipative, the DS and LASD models can account for backscatter, but only by computing locally small or even negative eddy viscosity coefficients, an approach which, in addition to being nonphysical, can result in numerical instability in the absence of additional sources of dissipation.

Several nonlinear SFS stress models have appeared in the literature that account for some or all of the above-discussed deficiencies of the linear eddy viscosity models. Two such approaches have been implemented into the WRF model for examination.

The first nonlinear model used in this study is the Nonlinear Backscatter and Anisotropy SFS stress model (NBA) of Kosović, given by

$$M_{ij} = -(C_S l)^2 \left\{ 2\left(2\widetilde{S_{mn}}\widetilde{S_{mn}}\right)^{\frac{1}{2}}\widetilde{S_{\imath J}} + C_1\left(\widetilde{S_{\imath k}}\widetilde{S_{kJ}} - \frac{1}{3}\widetilde{S_{mn}}\widetilde{S_{mn}}\delta_{ij}\right) + C_2\left(\widetilde{S_{\imath k}}\widetilde{R_{kJ}} - \widetilde{R_{\imath k}}\widetilde{S_{kJ}}\right)\right\} \quad (10)$$

Here $\widetilde{R_{\imath J}} = \frac{1}{2}\left(\frac{\partial \widetilde{u_\imath}}{\partial x_j} - \frac{\partial \widetilde{u_J}}{\partial x_i}\right)$ is the rotation rate tensor, and C_S, C_1 and C_2 are model parameters that are formulated in terms of a backscatter coefficient, which reduces the overall dissipation. The model parameters ensure that the proper misalignment between the eigenvectors of the stress and strain rate tensors is preserved for sheared homogeneous turbulence.

The second nonlinear model implemented into WRF is the Dynamic Reconstruction Model (DRM) of Chow et al. (2005). This is a two-part SFS stress model, consisting of both a dynamic eddy-viscosity component (computed following Wong and Lilly (1994), which is similar to the DS model), and a component denoted the resolvable subfilter-scale (RSFS) stress. The RSFS stresses are computed using explicit filtering and reconstruction, which involves both the forward and inverse application of a filter. The procedure begins with reconstruction of the RSFS velocities, $\widetilde{u_\imath}$, from the resolved velocities $\overline{\widetilde{u_\imath}}$. Here the overbar denotes the explicit filter, while the tilde denotes filtering implicitly provided by the numerical mesh. The prognostic velocities computed using the DRM model are considered to have been explicitly filtered, due to the use of the filter in the computation of the RSFS stresses, which force the flow. The RSFS velocities are obtained by inverting the filter operator, using the approximate deconvolution method of Stoltz and Adams (1999). Once $\widetilde{u_\imath}$ are obtained, the RSFS stresses are computed from the forward application of the filter to the RSFS velocities, $\tau_{ij}^{RSFS} = (\overline{\widetilde{u_i^*}\widetilde{u_j^*}} - \overline{\widetilde{u_i^*}}\,\overline{\widetilde{u_j^*}})$. The asterisk indicates that a truncated series expansion for the filter inverse has been used.

In contrast to the stresses provided by the eddy viscosity model, the RSFS stresses are not absolutely dissipative, and its eigenvectors are not generally aligned with those of the strain rate tensor, analogous to the nonlinear terms in the NBA model.

When using lower-order computational methods, the increased numerical errors near the surfaces can result in the dynamic procedure providing too little dissipation. One solution is to implement an additional near-wall stress model to ameliorate the stresses deficit. (Chow et al, 2005). The DRM model uses the near-wall stress model of Brown et al. (2001), given by

$$\tau_{i3} = -\int_0^z C_c a(z)|\bar{\tilde{u}}|\bar{\tilde{u}}_i dz, \quad (11)$$

where $i = 1,2$, C_c is a scaling factor, and $a(z)$ is the shape function. This near-wall stress model is also used with the LASD model which, when implemented into WRF, likewise requires augmentation of the near-surface stress field.

3 WRF SIMULATION SETUP

This study examines impacts on the accuracy of nested large-eddy simulations in the WRF model due to errors arising from the transition of the flow across the nest interface, and from the more coarsely-resolved bounding simulations providing the boundary conditions for the nested simulation. To isolate these effects, we begin with a simplified configuration for which these errors can be isolated and quantified. We utilize a simulation using one nested domain contained

within a bounding simulation. The outer domain (d01) has a size of approximately 12 x 8 x 1 km, using 151 x 101 x 48 gridpoints in x-, y- and z- directions. The nested domain (d02) is approximately 10 x 6 x 1 km and uses 361 x 241 x 48 gridpoints in x-, y- and z- directions. Vertical grid spacing on both domains is 6.75 m at the surface, stretched by approximately 5% per nodal index aloft. The horizontal grid spacing is 81 m for d01 and 27 m for d02.

We examine neutral, boundary-layer flow over a flat, rough surface. The simulations are forced with a uniform geostrophic wind aligned along the x-axis, with a magnitude of 10 m/s. The surface boundary condition is a standard logarithmic similarity function, with a surface roughness of 0.1 m. While the nested domain receives its boundary conditions from the outer domain solution, the outer domain solution utilizes periodic lateral boundary conditions.

The accuracy of the nested domain solution is ascertained using comparison against a separate, single-domain solution with the same computational mesh as that of the nested domain, but using periodic lateral boundary conditions (d02S). In the absence of errors from the nest interface and bounding flow, the solution on the nested domain should be statistically identical to the stand-alone simulation. Therefore any differences in flow statistics between those simulations are attributable to errors arising from either the transition of flow across the nest, or from the bounding domain solution itself. We are mainly interested in the evolution of flow beyond the coarse-to-fine interface as the flow enters the nest, as opposed to the fine-to-coarse interface as the flow exits, as we envision applications with the site of interest in the nest.

4 RESULTS

Figure 1 depicts the configuration of the domains and shows a snapshot of simulated flow fields on both the outer (d01, left) and nested (d02, middle) domains of the nested simulation, as well as for the stand-alone (d02S, right) simulation. The color contours are of the zonal component of the velocity, and each solution is shown at a height of 102 m above the surface. The location of the nested domain within the bounding domain is shown by the dotted rectangle.

Readily apparent is the profound difference in the flow between d01 and d02S, both of which use periodic lateral boundary conditions, but which utilize mesh resolutions separated by a factor of three. First, as expected, smaller-scale features are observed in d02S, due to the smaller grid spacing. However, surprisingly the largest structures predicted on each mesh also differ markedly, with the regions of high spatial correlations covering much larger distances in d01, than d02S. Also apparent is the evolution of the flow within the d02, the morphology of which increasingly resembles that of the d02S as it traverses the nest. Specifically the flow develops both reduced spatial correlations and smaller-scale structures with increasing distance through the nested domain.

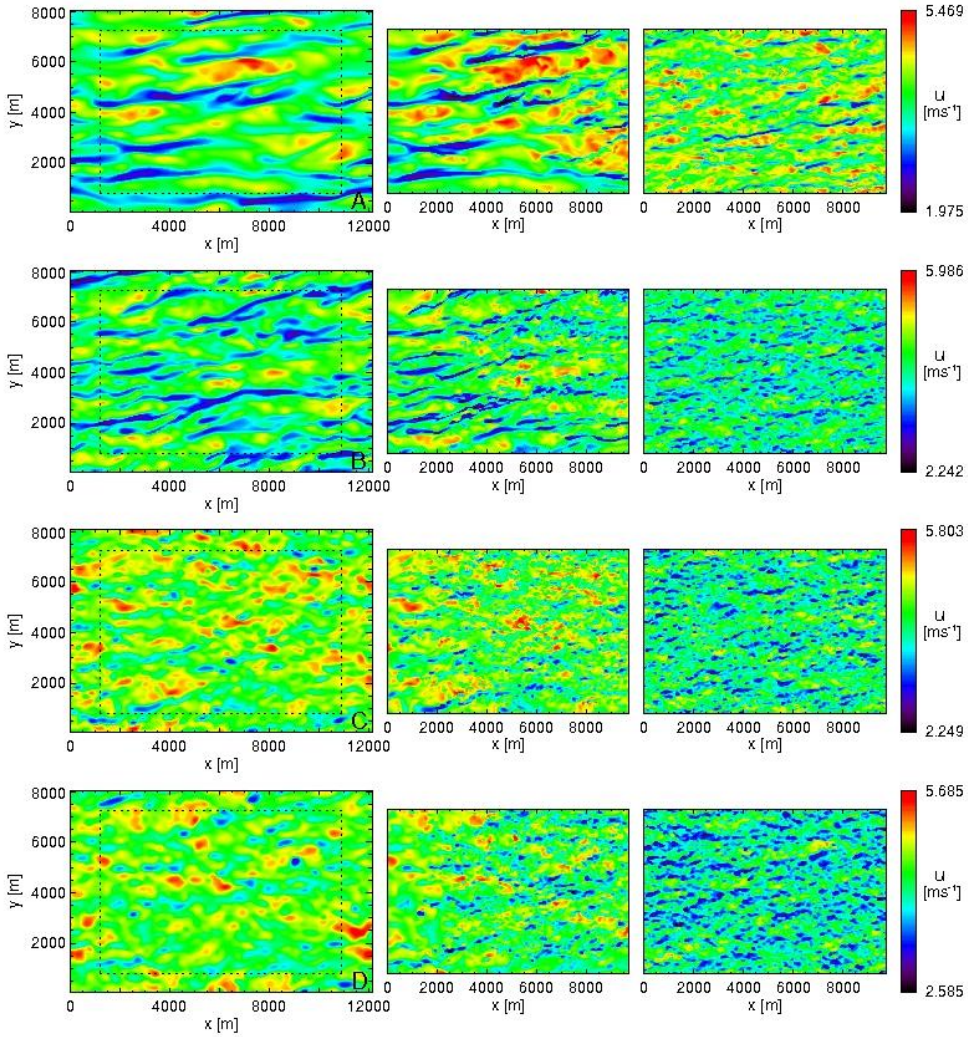

Figure 1. Contours of u-velocity at z=102 m in d01 (left), d02 (middle) and d02S (right) domains; a) SS model; b) NBA model; c) LASD model; d) DRM model.

Figure 2 shows same contours as Fig. 1, but at the first model gridpoint above the surface, z=3.4 m. Here the differences between both the different domains and among the different SFS stress models are much more pronounced. Of particular importance is how differently the SFS stress models influence the flow equilibration process at the nest boundaries. In simulations using SS and NBA models (Fig. 2a,b), generation of small scale structures is delayed, with each model predicting very long streaks in d02 which differ markedly from those predicted on both d01 and d02S. The dynamic models (Fig. 2c,d), feature a much more rapid recovery due to the variable constant in the eddy viscosity, which can decrease the dissipation upon entry of the flow into the nest, allowing smaller scales of turbulence to develop more quickly.

The reduction in flow velocity near the surface at the d02 inflow interface is caused by a mismatch between the SFS stresses computed above the surface, relative to their parameterized values applied at the surface. The lack of resolved structure within the flow as the flow enters d02 results in very small stresses above the surface. The surface stresses, which are parameterized as a function of the velocity magnitude, are much larger, yielding a vertical stress divergence that retards the flow.

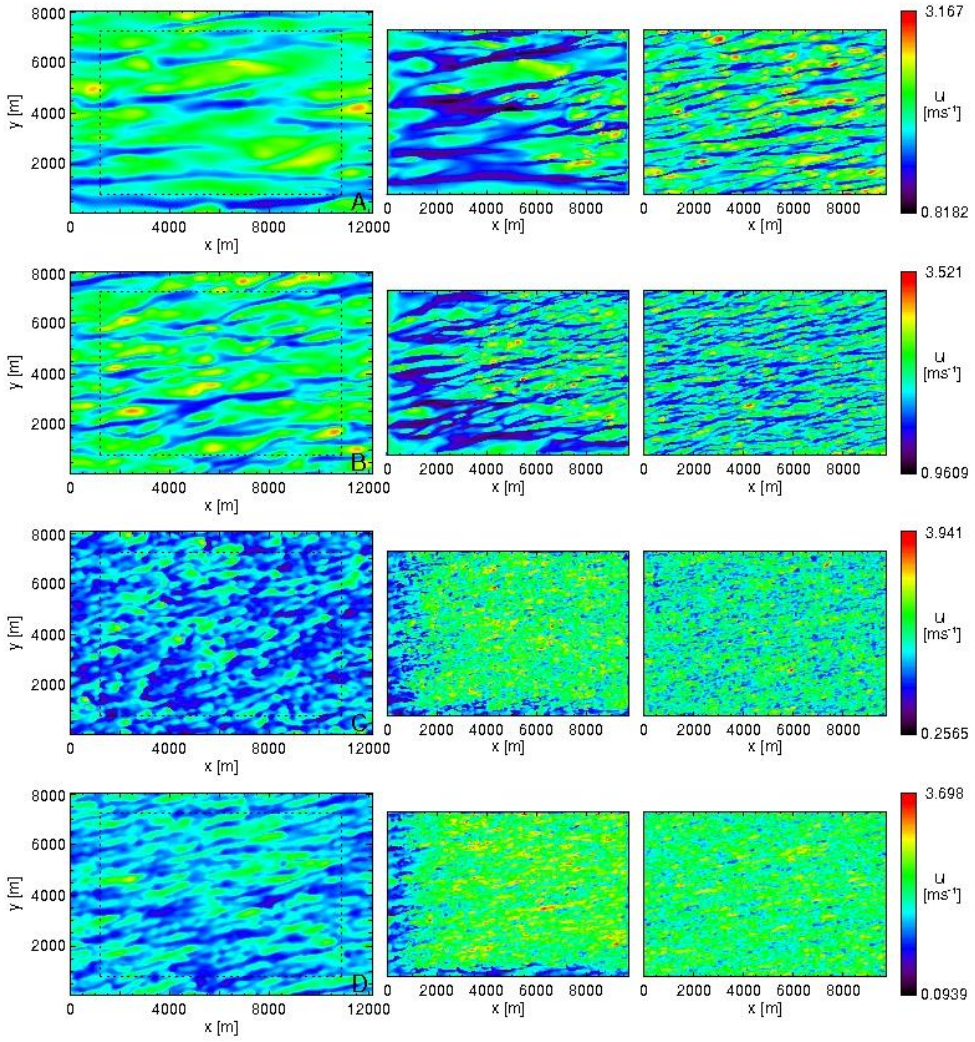

Figure 2. Contours of u-velocity at z=3.4 m. in d01 (left), d02 (middle) and d02S (right) domains; a) SS model; b) NBA model; c) LASD model; d) DRM model.

5 CONCLUSION

In this study, we investigated the flow equilibration process at the inflow nest interfaces using WRF model simulations of neutral, geostrophically-forced boundary-layer flow over a flat, rough surface. We compared the nested solution, which receives its lateral boundary condition from a coarser-resolution bounding simulation, with a stand-alone simulation which has the same resolution as the nested domain. We examined the performance of four different SFS stress models, a static linear eddy-viscosity model (SS), a nonlinear model (NBA), a dynamic linear eddy-viscosity model (LASD), and a mixed dynamic linear eddy viscosity and nonlinear scale similarity model (DRM). We observe considerable discrepancies in nested solutions relative to their stand-alone equivalents in the near-surface flow near the nest inflow interfaces. While each of the simulations exhibit sharp reductions in mean velocity near the surface at the nest inflow, the two dynamic model simulations are able to recover more quickly than those from the other mod-

els, due to the ability of the dynamic models to compute very small eddy viscosity coefficients, allowing for the rapid creation of resolved structures within the flow.

Future work will entail modification of the surface stress parameterization to circumvent the stress divergence that causes the rapid retardation of the flow, and the exploration of a grid-independent length scale formulation to potentially ameliorate the effects of the sharp discontinuity in the presently formulated length scale that occur at the nest interface.

6 ACKNOWLEDGEMENTS

We thank Elie Bou-Zeid, Tina Katopedes Chow and Branko Kosovic for their help in implementing the sub-grid scale models used in this paper. This work is performed under the auspices of Department of Energy by Lawrence Livermore National Laboratory under contract DE-AC52-07NA27344. LLNL-xxxxx.

7 REFERENCES

Brown, A. R., Hobson, J. M. and Wood, N., 2001. Large Eddy Simulation of neutral turbulent flow over rough sinusoidal ridges. Boundary Layer Meteorology, 98, 411-441.

Bou-zeid, E., Meneveau, C. and Parlange, M. B., 2005. A scale-dependent Lagrangian dynamic model for large eddy simulation of complex turbulent flows. Physics of Fluids, 17, 025105.

Chow, F. K., Street, R. L., Xue, M. and Ferziger, J. H., 2005. Explicit filtering and reconstruction turbulence modeling for large-eddy simulation of neutral boundary layer flow. J. Atmos. Sci., 62, 2058-2077.

Germano, M., Piomelli, U., Moin, P. and Cabot, W. H., 1991. A dynamic subgrid-scale eddy viscosity model. Physics of Fluids A, 3, 1760-1765.

Hatlee, S. C. and Wyngaard, J. C., 2007. Improved subfilter-scale models from the HATS field data. J. Atmos. Sci., 64, 1694-1705.

Keating, A., Piomelli, U., Balaras, E. and Kaltenbach, H.-J., 2004. A priori and a posteriori tests of inflow conditions for large-eddy simulation. Phys. of Fluids, 16 (12), 4696-4712.

Kelly. M., J. C. Wyngaard, and Sullivan, P. P., 2009. Application of a subfilter-scale flux model over the ocean using OHATS field data. J. Atmos. Sci, submitted.

Kosovic, B., 1997. Subgrid-scale modeling for the large-eddy simulation of high-Reynolds number boundary layers. J. Fluid Mechanics, 336, 151-182.

Meneveau, C., Lund, T. and Cabot, W., 1996. A Lagrangian dynamic subgrid-scale model of turbulence. J. Fluid Mechanics, 319-353.

Piomelli, U., Kang, S., Ham, F. and Iaccarino, G., 2006. Effect of discontinuous filter width in large-eddy simulations of plane channel flow. Proc. Center for Turbulence Research Summer Program 2006, Stanford University.

Porte-Agel, F., Meneveau, C. and Parlange, M. B., 2000. A scale dependent dynamic model for large eddy simulation: application to a neutral atmospheric boundary layer. J Fluid Mechanics, 415, 261-284.

Skamarock, W. C, Klemp, J. B., Dudhia, J., Gill, D. O., Barker, D. M., Duda, M. G., Huang, Xiang-Y., Wang, W. and Powers, J. G., 2008. A description of the Advanced Research WRF Version 3. NCAR Technical Note.

Stolz, S. and Adams, N. A., 1999. An approximate deconvolution procedure for large-eddy simulation. Physics of Fluids, 11, 1699-1701.

Vanella, M., Piomelli, U. and Balaras, E. 2008. Effect of grid discontinuities on large-eddy simulation statistics and flow fields. J. of Turbulence, 9 (32), 1-23.

Wong, V. C. and Lilly, D. K., 1994. A comparison of two dynamic subgrid closure methods for thermal-convection. Physics of Fluids, 6, 1016-1023.

Wyngaard, J.C., 2004. Toward Numerical Modeling in the “Terra Incognita”. J. Atmos. Sci., 61, 1816-1826.